

FEASIBILITY STUDY ON IMPROVING ARRIVAL-SEPARATION STABILITY THROUGH ARRIVAL TRAJECTORY ANALYSIS AT CONGESTED AIRPORTS

Ryo Kajikawa[1], Noboru Takeichi[1]

[1] Graduate School of Systems Design, Tokyo Metropolitan University, Japan

Abstract

The Point Merge System (PMS) has been widely adopted at major airports to streamline arrival management. However, in PMS operations at Haneda Airport, no procedural speed and altitude restriction are specified for a portion of the segment after the sequencing leg, which may cause trajectory variability and fluctuating arrival separation. This study analyzes actual operational data from consecutive landing pairs to evaluate the relationship between trajectory variability and arrival-separation variability while reducing the influence of wind conditions by focusing on consecutive landing pairs. Functional Principal Component Analysis (FPCA) and Ward's hierarchical clustering are applied to altitude and calibrated airspeed (CAS) profiles in the segment without procedural speed and altitude restriction. The analysis identifies low-variability clusters in which arrival-separation variability is reduced and the rate of insufficient separation under RECAT is approximately halved compared with the overall dataset. This reduction in variability suggests the potential to reduce arrival-separation while maintaining the same level of safety, or alternatively, to reduce the probability of insufficient separation under the current spacing operation. Furthermore, the analysis of time-interval variance shows that spacing adjustment on the sequencing leg is the main factor reducing arrival-separation variability, while the effect of speed adjustment after leaving the sequencing leg is relatively limited.

Keywords: Air Traffic Management, Trajectory Data Analysis, Point Merge System

1. Introduction

Although global air travel demand temporarily declined following the worldwide outbreak of COVID-19, air traffic demand has since recovered substantially. In Japan, domestic passenger traffic had already exceeded the pre-pandemic level by FY2023 [1]. In addition, the number of arriving aircraft at Tokyo International Airport, hereafter referred to as Haneda Airport, the largest airport in Japan, exceeded 650 per day in FY2024 [2]. According to the Civil Aviation Bureau, runway capacity at the airports in the Tokyo metropolitan area, namely Haneda and Narita Airports, is expected to become increasingly constrained in the future. Therefore, the medium- and long-term enhancement of airport functions in the Tokyo metropolitan area has been identified as a key policy priority. In Japan, Collaborative Actions for Renovation of Air Traffic Systems 2040 (CARATS 2040) has been formulated as a long-term vision for the future air traffic system. This vision sets out six goals for achieving a convenient and sustainable air traffic system, with safety as the highest priority [3]. Against this background, the Point Merge System (PMS) [4], shown in Figure 1, was introduced into the terminal airspace of Haneda Airport as a systemized method for sequencing arrival flows and mitigating arrival congestion [5]. The PMS is a systemized method developed by EUROCONTROL for sequencing arrival flows toward the runway. It is expected to improve arrival management efficiency and reduce controller workload. As shown in Figure 1, the PMS consists of arc-shaped sequencing leg, hereafter referred to as Leg, and a Merge Point (MP), where arrival flows converge. When the separation from a preceding aircraft at the MP is expected to become insufficient, the following aircraft can be kept on the Leg to extend its path and increase the separation. In Japan, PMS is used to adjust the spacing of arrival traffic at Haneda Airport, the country's busiest airport by passenger volume, as well as at Narita, Fukuoka, and Kansai International Airports.

A previous study [6] reported that, in PMS operations at Haneda Airport, aircraft exhibit variations in altitude and calibrated airspeed (CAS). Since these variations affect flight-time variability and, consequently, arrival-separation variability, reducing trajectory variability is expected to contribute to landing capacity enhancement. In the PMS, procedural speed and altitude restriction are specified on

the Leg and at points 5 NM and 10 NM from the runway threshold. However, no procedural speed and altitude restriction are specified between the Leg and APOLO. The authors' previous study [7] focused on the section after APOLO, where procedural speeds are specified, and showed that reducing speed variability may contribute to landing capacity enhancement. In contrast, the present study focuses on the altitude and CAS profiles from the Leg exit to APOLO, where no procedural speed and altitude restriction are specified. Through this analysis, the study evaluates the potential reduction in arrival-separation variability and the feasibility of landing capacity enhancement through the introduction of procedural speed and altitude restriction between the Leg and APOLO.

For the analysis of flight trajectories, clustering-based approaches have been widely used as data-driven methods for aircraft trajectory data. Representative studies include the detection of anomalous trajectories based on spatial and energy-based indicators [8], the identification of trajectory patterns in complex terminal airspace and their application to arrival-time prediction using features such as time, position, altitude, heading, horizontal speed, and vertical speed [9], and an airspace monitoring method based on principal component analysis of trajectories [10]. In the present study, clustering is also used to extract representative trajectory patterns. Specifically, actual operational data from aircraft operating under PMS procedures at Haneda Airport are analyzed, with a focus on consecutive arriving aircraft pairs to reduce the influence of wind on flight time. Clustering is then applied to extract representative trajectory patterns with small altitude and CAS variability from the Leg exit to APOLO. This enables an evaluation of whether such trajectories can contribute to reducing arrival-separation variability and potentially reducing arrival separation while maintaining the same level of safety. Furthermore, by focusing on changes in the time-interval variance between preceding and following aircraft in each cluster, this study quantitatively analyzes which segments within the PMS contribute to the reduction of spacing variability.

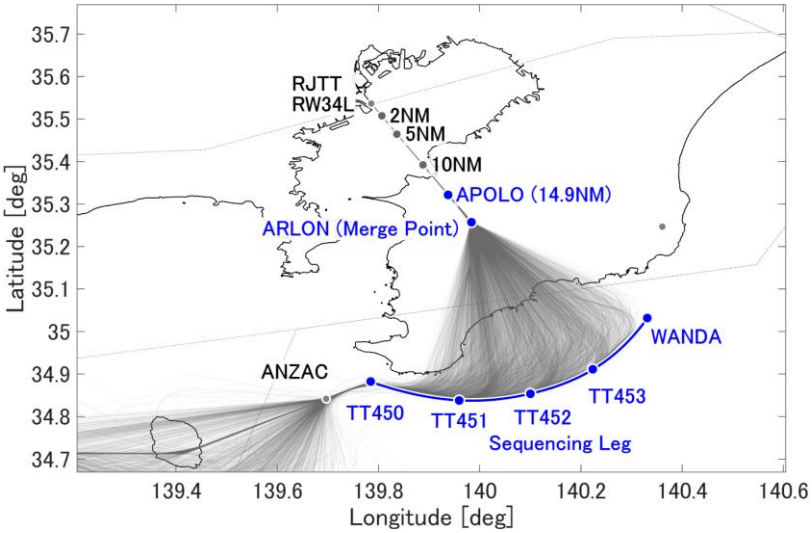


Figure 1 – Overview of the Point Merge System arrival route.

2. Data Used in This Study

2.1 Flight Data

Operational flight data provided by the OpenSky Network [11] were used in this study. These data consist of Automatic Dependent Surveillance–Broadcast (ADS-B) and Mode S signals transmitted from aircraft, and include state information such as latitude, longitude, altitude, ground speed, and aircraft type at 1-second intervals. The analysis used OpenSky Network data collected from January 1, 2022, to December 31, 2025. To satisfy the objective of this study, flights operating in PMS arrivals at Haneda Airport were extracted from the dataset. Among these flights, pairs of consecutive aircraft landing on RW34L were extracted, and each pair was defined as a preceding aircraft and its following aircraft.

Since CAS is not directly included in the OpenSky Network data, it was calculated using aircraft state information and meteorological data obtained from the MSM dataset [12]. Meteorological data corresponding to the aircraft position and time were first obtained from the MSM dataset. The TAS vector was then obtained by subtracting the wind vector from the ground-speed vector, and TAS was calculated as its magnitude. Subsequently, TAS was converted into CAS using the atmospheric density estimated from the pressure altitude of each aircraft and the outside air temperature obtained from the MSM data.

2.2 Meteorological Data

Meteorological fields were taken from the Meso Scale Model (MSM) dataset [12] provided by the Japan Meteorological Agency. In this study, the most recent MSM forecast available prior to each aircraft record time was used, and meteorological variables at the aircraft position were estimated by linear interpolation in time, longitude, latitude, and pressure level. The pressure level was calculated from the pressure altitude of each aircraft. The MSM dataset covers the region surrounding Japan, spanning from 20°N to 48°N latitude and from 120°E to 150°E longitude. The data are provided on a grid with a temporal resolution of 3 hours, a latitudinal resolution of 0.1°, and a longitudinal resolution of 0.125°.

2.3 RECAT

RECAT (Recategorization of Wake Turbulence Separation Minima) was used as the evaluation metric for arrival spacing. RECAT is a wake turbulence separation standard established to optimize the management of wake turbulence effects during takeoff and landing operations by categorizing aircraft based on wake turbulence characteristics [13]. As shown in Table 1, aircraft are classified into seven categories, and the required separation distance is determined according to the combination of preceding and following aircraft categories. Compared with conventional wake turbulence separation standards, RECAT provides more finely categorized separation criteria, enabling more flexible and efficient arrival operations.

Table 1 – RECAT.

Unit: [NM]		Following aircraft						
		A	B	C	D	E	F	G
Preceding aircraft	A		4	5	5	6	6	8
	B		3	4	4	5	5	7
	C				3	3.5	3.5	6
	D							4
	E							4
	F							
	G							

Group	Maximum Take-Off Weight [kg]	Wingspan [m]
A	$136{,}000 \leq \mathrm{M}$	$74.68 < s \leq 80$
B		$53.34 < s \leq 74.68$
C		$38.1 < s \leq 53.34$
D	$186{,}000 \leq \mathrm{M} < 136{,}000$	$32 < s$
E		$27.43 < s \leq 32$
F		$s \leq 27.43$
G	$\mathrm{M} \leq 186{,}000$	-

2.4 Aeronautical Information Publication (AIP)

The Aeronautical Information Publication (AIP) published by the Japan Civil Aviation Bureau provides operational information such as arrival routes, altitude restrictions, and procedural speed. In this study, the prescribed PMS trajectories implemented at Haneda Airport were defined based on the AIP [14]. Figure 2 shows the Standard Terminal Arrival Route (STAR) at Haneda Airport corresponding to the PMS, which include arc-shaped arrival paths.

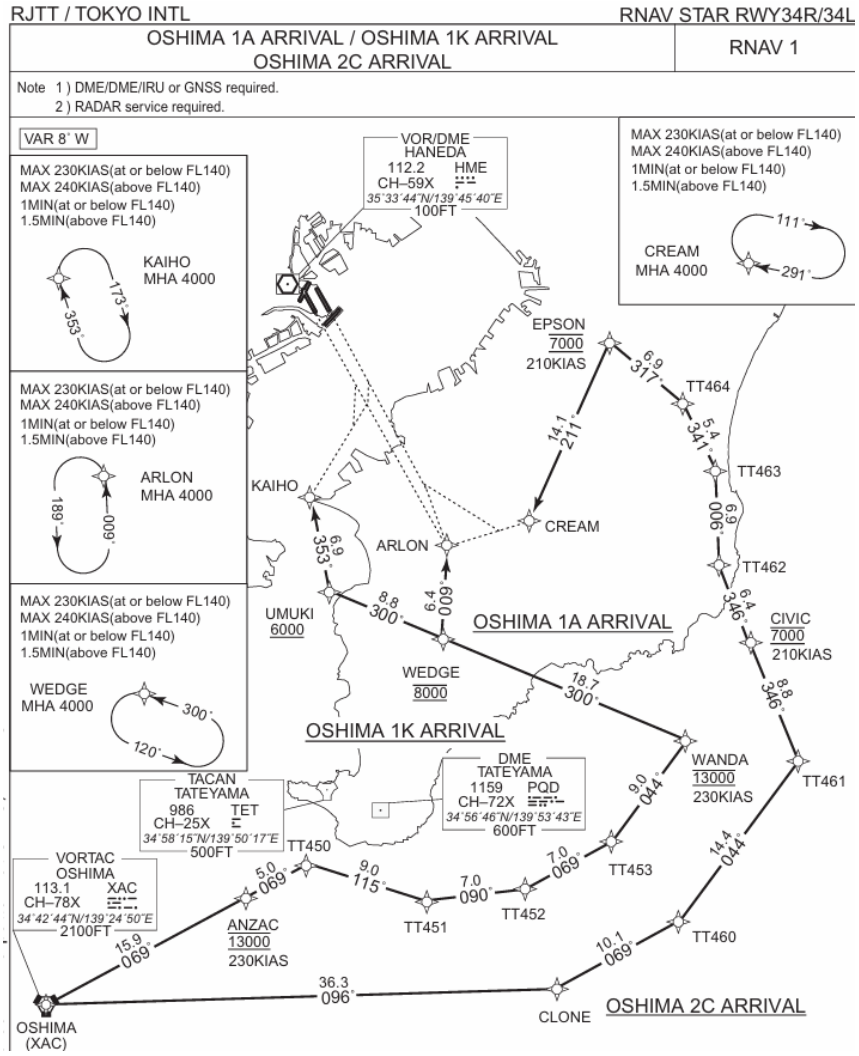


Figure 2 – STAR corresponding to the PMS at Haneda Airport [14].

3. PMS Arrival Operations

In PMS operations, aircraft arriving at RW34L at Haneda Airport fly in accordance with Standard Terminal Arrival Routes (STARs) [14]. In this study, flights following the OSHIMA 1A ARRIVAL STAR, which was the most frequently observed PMS arrival route for RW34L in the dataset, were selected as the analysis target. Among these flights, aircraft that proceeded directly from the Leg to ARLON, the Merge Point (MP), were extracted for analysis. Figure 1 shows the horizontal tracks of the extracted flights operating on the target route. According to the Aeronautical Information Publication (AIP), an altitude constraint of 13,000 ft and a procedural speed of 230 kt are specified for the section from TT450 to WANDA, which corresponds to the Sequencing Leg (Leg) of the OSHIMA 1A ARRIVAL. After passing APOLO, procedural speeds of 180 kt and 160 kt are specified at points 10 NM and 5 NM from the runway threshold, respectively [14]. Table 2 presents an excerpt from the AIP showing the altitude and calibrated airspeed (CAS) constraints for the OSHIMA 1A ARRIVAL.

Table 2 – Procedure-specified altitude and speed constraints

Waypoint/Distance from Threshold	Altitude (FT)	Speed (KCAS)
ANZAC	13000	230
TT450	-	-
TT451	-	-
TT452	-	-
TT453	-	-
WANDA	13000	230
10 NM	Not specified	180
5 NM	Not specified	160

Figures 3(a) and 3(b) show the corresponding altitude profiles and calibrated airspeed (CAS) profiles, respectively. Figures 3(c) and 3(d) show the corresponding altitude-difference and CAS-difference profiles between preceding and following aircraft, respectively. The black lines in the figures indicate the 5th and 95th percentiles, and approximately 90% of the data lie within this range. The 38 NM point shown in the figures was selected because all aircraft included in the analysis had exited the Leg before reaching this point. Therefore, the 38 NM point and TT450 were defined as the endpoints of the section for each flight Accordingly, in this section, the horizontal axis is normalized so that the profile shapes of different flights can be compared. In contrast, for the section closer to the runway than 38 NM, each profile is shown based on the distance from the runway threshold. These figures show that large variations exist in both altitude and CAS profiles in the section from 38 NM to APOLO, where no published altitude or speed restrictions are specified.

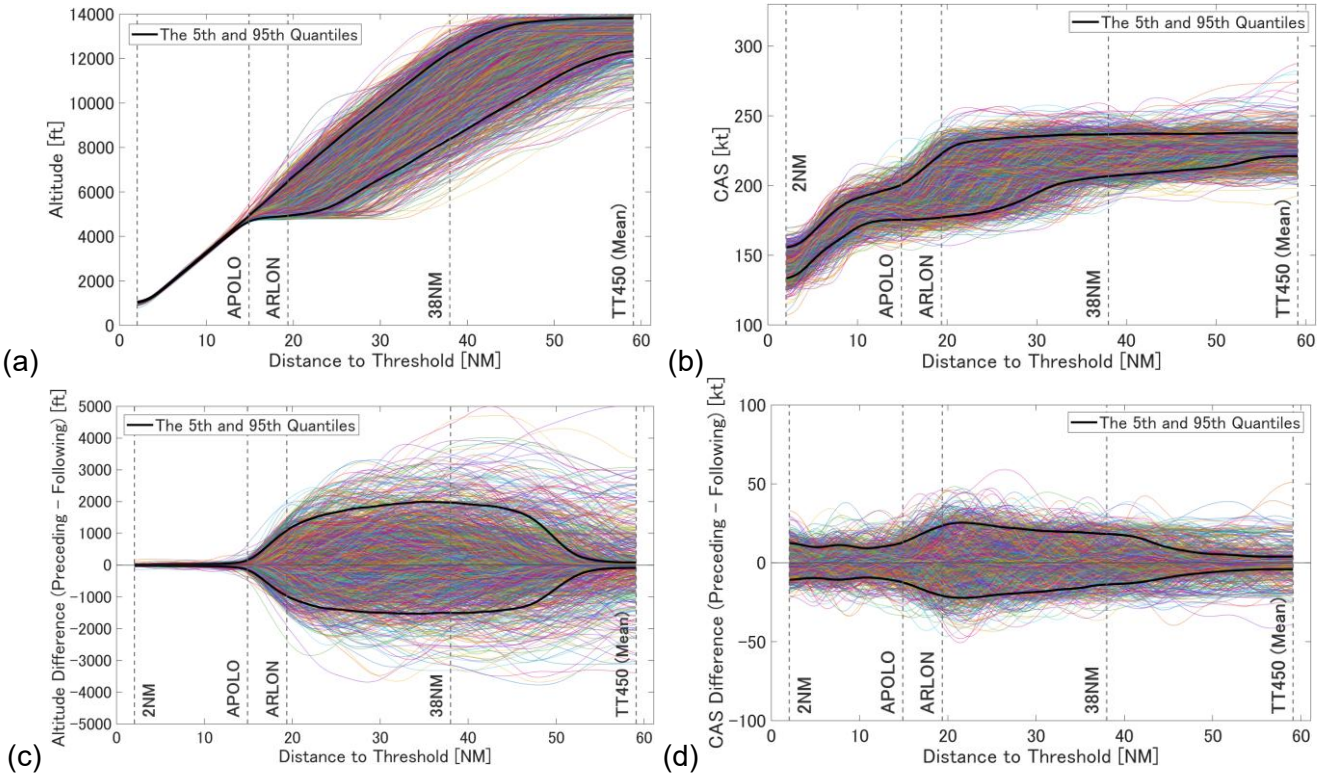


Figure 3 – Trajectory profiles of aircraft operating under PMS procedures:
(a) altitude profiles, (b) CAS profiles, (c) altitude-difference profiles, and (d) CAS-difference profiles.

4. Analysis of Operational Data

4.1 Analysis Methodology

Currently, no explicit altitude or calibrated airspeed (CAS) profiles are prescribed for the segment between the sequencing leg (Leg) and the APOLO in PMS operations at Haneda Airport. In this study, representative altitude and CAS profiles commonly observed among flights are extracted from operational trajectory data. If the variability of these representative operational profiles is smaller than that observed across the overall flight population, establishing such profiles as reference operational profiles may contribute to reducing trajectory variability in actual operations. Functional Principal Component Analysis (FPCA) [15] was applied in this study. FPCA is a dimensionality reduction method that extracts the dominant modes of variation shared among flight trajectories. The application of FPCA enables efficient analysis focusing on the principal characteristics of flight trajectories. Subsequently, clustering analysis based on a Ward's method [16] was performed using the principal component scores obtained from FPCA as feature vectors. Through this process, groups of flights exhibiting similar operational profiles were extracted.

4.2 Analysis of Flight Trajectory Data

4.2.1 Consecutive Arrival Pairs

In this study, 1582 consecutive arrival pairs with a RECAT separation minimum of 3 NM were analyzed. These pairs were identified by matching the ICAO24 codes and callsigns of flights operating within the PMS with those of all arrivals to Runway 34L and confirming that the aircraft landed consecutively. The analysis focuses on consecutive arrival pairs in order to reduce the influence of wind conditions. Each pair consists of a preceding aircraft and a following aircraft that landed consecutively on RW34L. Since consecutive arrival aircraft are expected to operate under nearly identical wind conditions, the influence of wind variability can be substantially reduced. In addition, PMS operations are commonly used during peak traffic periods, enabling a large number of consecutive arrival pairs to be obtained. Figure 4 shows the distribution of arrival separation margins, defined as the actual arrival spacing minus the RECAT minimum separation of 3 NM, at 2 NM from the runway threshold for all analyzed aircraft pairs.

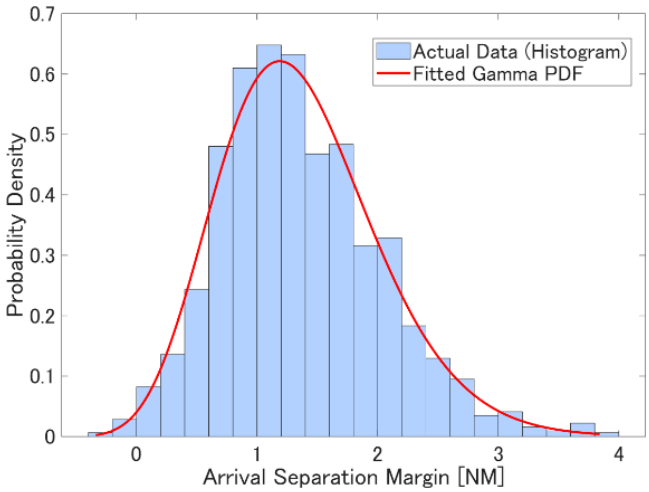


Figure 4 – Distribution of arrival separation margins and fitted gamma PDF for the overall dataset.

Based on the observed distribution, the arrival separation margins were modeled using a three-parameter gamma distribution, defined as follows: where k, θ, and c represent the shape, scale, and location parameters, respectively.

$$f(x;k,\theta,c) = \frac{(x-c)^{k-1} \cdot e^{-(x-c)/\theta}}{\Gamma(k) \cdot \theta^{k}} \quad (1)$$

The parameters were estimated using maximum likelihood estimation. Subsequently, goodness-of-fit was assessed using a bootstrap-corrected Kolmogorov–Smirnov test. The results summarized in Table

3 indicate that the analyzed reasonably represented by a gamma distribution. Gamma distributions have also been applied in previous studies to model arrival spacing distributions under congested traffic conditions [17]–[19].

Table 3 – Gamma distribution fitting results for arrival-separation margins.

pairs	k	θ	c	D
1582	14.0	0.18	-1.1	0.019

4.2.2 Functional Principal Component Analysis

In this study, Functional Principal Component Analysis (FPCA) was applied to altitude and calibrated airspeed (CAS) profiles. First, the trajectory data were smoothed and represented as continuous functions using B-spline basis functions. Principal component analysis was then applied to the resulting functional data. FPCA is a dimensionality reduction method that extracts the dominant modes of variation shared among functional trajectory datasets and has also been applied to aircraft trajectory analysis in previous studies [20][21]. Each trajectory was represented as a function of the distance from the runway threshold d. Altitude $alt(d)$ and calibrated airspeed $cas(d)$ profiles were then used to construct feature functions describing the characteristics of consecutive arrival pairs.

4.2.3 Ward's method

In this study, hierarchical clustering using Ward's method was applied to identify clusters with low trajectory variability that could serve as operationally feasible reference profiles for procedural speed and altitude restriction. Specifically, the analysis focused on trajectory data with small variations in altitude and CAS profiles. Ward's method is an agglomerative hierarchical clustering method in which each data point is initially treated as a separate cluster, and clusters are successively merged to minimize the increase in the within-cluster sum of squares. Since this method does not require a specific probabilistic distribution model to be assumed in advance, it is suitable for clustering the trajectory data considered in this study. In addition, because Ward's method merges clusters by minimizing the increase in the within-cluster sum of squares, it tends to form clusters with similar features and small within-cluster variability in the feature space. Ward's method has also been widely used in the analysis of aircraft trajectory data [22][23].

In this study, clustering was performed by treating two consecutive arriving aircraft as one pair. Therefore, to extract groups of trajectory data with common dominant variations, it is desirable to form clusters consisting of pairs in which the two aircraft have similar trajectory profile. For this reason, the differences and summed characteristics of the trajectories of two consecutive arriving aircraft were considered. FPCA was then applied to the following four feature functions, and the PCA scores from the first to fourth principal components were used as clustering features.

$$y_1(d) = alt_1(d) + alt_2(d) \tag{2}$$

$$y_2(d) = |alt_1(d) - alt_2(d)| \tag{3}$$

$$y_3(d) = cas_1(d) + cas_2(d) \tag{4}$$

$$y_4(d) = |cas_1(d) - cas_2(d)| \tag{5}$$

This approach aims to form clusters of aircraft pairs with similar trajectories in terms of both the differences and sums of the speed profiles of the preceding and following aircraft. Among these clusters, it is expected that some clusters will consist of a large number of aircraft pairs in which the preceding and following aircraft exhibit nearly identical histories and similar altitude and speed profiles. The distance range (d) used for feature extraction was defined as the section from 14.9 NM to 38 NM from the runway threshold. This range was determined since APOLO is located 14.9 NM from the runway threshold and that all aircraft had exited the Leg by 38 NM from the runway threshold. Figure 5 shows the feature extraction range.

The appropriate number of clusters was determined based on the Calinski–Harabasz index (CH index)

[24]. The CH index is an internal clustering validation metric defined as the ratio of between-cluster variance to within-cluster variance, adjusted by the corresponding degrees of freedom. A larger CH index indicates better separation between clusters and smaller within-cluster variability. In this study, the hierarchical structure obtained using Ward's method was cut at each candidate number of clusters, and the CH index was calculated for each resulting partition. The number of clusters that maximized the CH index was then selected.

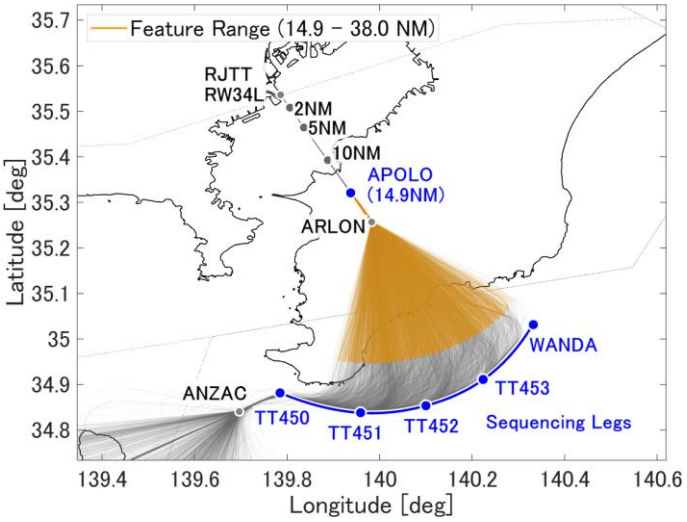


Figure 5 – Feature extraction range used for clustering (orange region).

4.2.4 Evaluation of Potential Arrival-Separation Reduction

Reducing trajectory variability may reduce arrival spacing variability, thereby enabling shorter arrival spacing while maintaining the current level of operational safety. To assess the feasibility of reducing arrival spacing, the arrival separation margins of each cluster were modeled using the previously described three-parameter gamma distribution. Goodness-of-fit was assessed using a bootstrap-corrected Kolmogorov–Smirnov test. The arrival separation margin $X$was defined as the difference between the actual arrival spacing measured at 2 NM from the runway threshold and the RECAT minimum separation of 3 NM. Let $S_{2\mathrm{NM}}$denote the actual arrival spacing between the preceding and following aircraft at 2 NM from the runway threshold:

$$X = S_{2NM} - 3\ \mathrm{NM} \tag{6}$$

The probability of insufficient arrival spacing for the overall dataset was then calculated using the following equation and used as the allowable safety criterion P_{ins}:

$$P_{ins,j} = P(X \le 0) = \int_{c_{\mathrm{all}}}^{0} f\left(x; k_j, \theta_j, c_j\right) dx \tag{7}$$

A three-parameter gamma distribution was then fitted to the arrival separation margin data for each cluster, yielding the cluster-specific parameters k_j, θ_j, and c_j. The quantile corresponding to the prescribed safety criterion $P_{\mathrm{ins}}$was then obtained from the inverse cumulative distribution function of the fitted distribution, as follows:

$$x_{\mathrm{target},j} = F^{-1}\left(P_{ins}; k_j, \theta_j, c_j\right) \tag{8}$$

The value of $x_{\mathrm{target},\,j}$represents the lower-tail quantile of the arrival separation margin distribution corresponding to the prescribed safety criterion for each cluster. The difference between the current mean separation margin and this quantile was then used to determine the allowable reduction in the mean separation margin. Letting the current mean separation margin be denoted by $\mu_{\mathrm{current},\,j}$, the target mean separation margin $\mu_{\mathrm{target},\,j}$is defined as follows:

$$\mu_{\mathrm{target},\,j} = \mu_{\mathrm{current},j} - x_{\mathrm{target},j} \tag{9}$$

In this study, the potential improvement in runway throughput was estimated by comparing the target mean separation margin $\mu_{\text{target},j}$ with the overall mean separation margin observed under current operations.

Trajectory variability within each cluster was quantified using the root-mean-square deviation from the corresponding cluster mean trajectory. Let $q_i(x)$ denote either the altitude trajectory $h_i(x)$ or the CAS trajectory $v_i(x)$ of the i-th aircraft and let $q_{mean,j}(x)$ denote the corresponding cluster mean trajectory. When the feature extraction interval is defined as $[a, b]$ and the number of aircraft in the cluster is N_j, the variability metric is defined as follows:

$$S_j(q) = \sqrt{\frac{1}{N_j}\sum_{i=1}^{N_j}\left(\frac{1}{b-a}\int_a^b \left(q_i(x) - q_{mean,j}(x)\right)^2 dx\right)} \tag{10}$$

This metric was computed separately for altitude and CAS trajectories to obtain $S(\text{Alt})$ and $S(\text{CAS})$, respectively. In addition, the difference between preceding and following aircraft trajectories within each cluster was quantified using the root-mean-square difference over the feature extraction interval. Let $q_{1,k}(x)$ and $q_{2,k}(x)$ denote the trajectories of the preceding and following aircraft in pair k, respectively, where q represents either altitude h or CAS v. When the feature extraction interval is defined as $[a, b]$ and the number of flight pairs in the cluster is M_j, the trajectory difference metric is defined as follows:

$$\Delta q_j = \sqrt{\frac{1}{M_j}\sum_{k=1}^{M_j}\left(\frac{1}{b-a}\int_a^b \left(q_{1,k}(x) - q_{2,k}(x)\right)^2 dx\right)} \tag{11}$$

By setting $q = h$ and $q = v$, the metrics ΔAlt and ΔCAS were obtained, respectively. Smaller values of these metrics indicate greater similarity between the preceding and following aircraft trajectories within the cluster.

5. Results

5.1 Results of Clustering

The results of the analysis are shown in Table 4. The RECAT insufficient rate for the overall dataset was $P_{\text{ins}} = 0.54\%$, and this value was used as the safety criterion. For the arrival-separation distribution of each cluster, the corresponding quantile, $x_{\text{target},j}$ was calculated using the inverse cumulative distribution function of the gamma distribution, and the target mean separation margin, $\mu_{\text{target},j}$, was then derived. Here, the variations in altitude and CAS within the feature extraction interval between APOLO and the 38 NM point from the runway threshold are denoted by $S(Alt)$ and $S(CAS)$, respectively. The mean altitude difference and CAS difference between preceding and following aircraft are denoted by ΔAlt and ΔCAS, respectively. In addition, P_{ins} represents the RECAT insufficient rate when the mean separation margin of the overall dataset is adjusted to match that of each cluster, and μ_{target} represents the target mean separation margin.

The analysis of consecutive arriving aircraft pairs showed that some clusters exhibited large differences in altitude and CAS profiles between preceding and following aircraft and high trajectory variability, whereas others exhibited similar trajectories and low trajectory variability. Cluster 1, which exhibited small variations in altitude and CAS, had a RECAT insufficient rate of $P_{ins} = 0.28\ \%$ and a target mean separation margin of $\mu_{\text{target}} = 1.29\ NM$. Both values were smaller than the corresponding values for the overall dataset, for which $P_{ins} = 0.54\%$ and $\mu_{\text{target}} = 1.37\ NM$. This indicates that, in clusters where the altitude and CAS profiles of preceding and following aircraft are similar, the variability of the arrival separation margin is reduced, allowing the mean separation margin to be reduced while satisfying the safety criterion. In contrast, Cluster 4 had the largest values, with $P_{ins} = 1.26\ \%$ and $\mu_{\text{target}} = 1.52\ \text{NM}$. This suggests that clusters with large variations in altitude and CAS profiles tend to have greater variability in the arrival separation margin.

Table 4 – Cluster-wise trajectory analysis results.

j	pairs	$S(Alt)$[ft]	$S(CAS)$[kt]	ΔAlt [ft]	ΔCAS [kt]	P_{ins} [%]	μ_{target} [NM]
All	1582	889.10	13.19	776.51	10.84	0.54	1.37
1	562	567.00	10.97	598.62	10.10	0.28	1.29
2	430	757.02	11.58	627.33	9.47	0.42	1.34
3	316	668.01	11.85	622.56	13.70	0.79	1.42
4	274	1071.13	13.13	1553.24	11.21	1.26	1.52

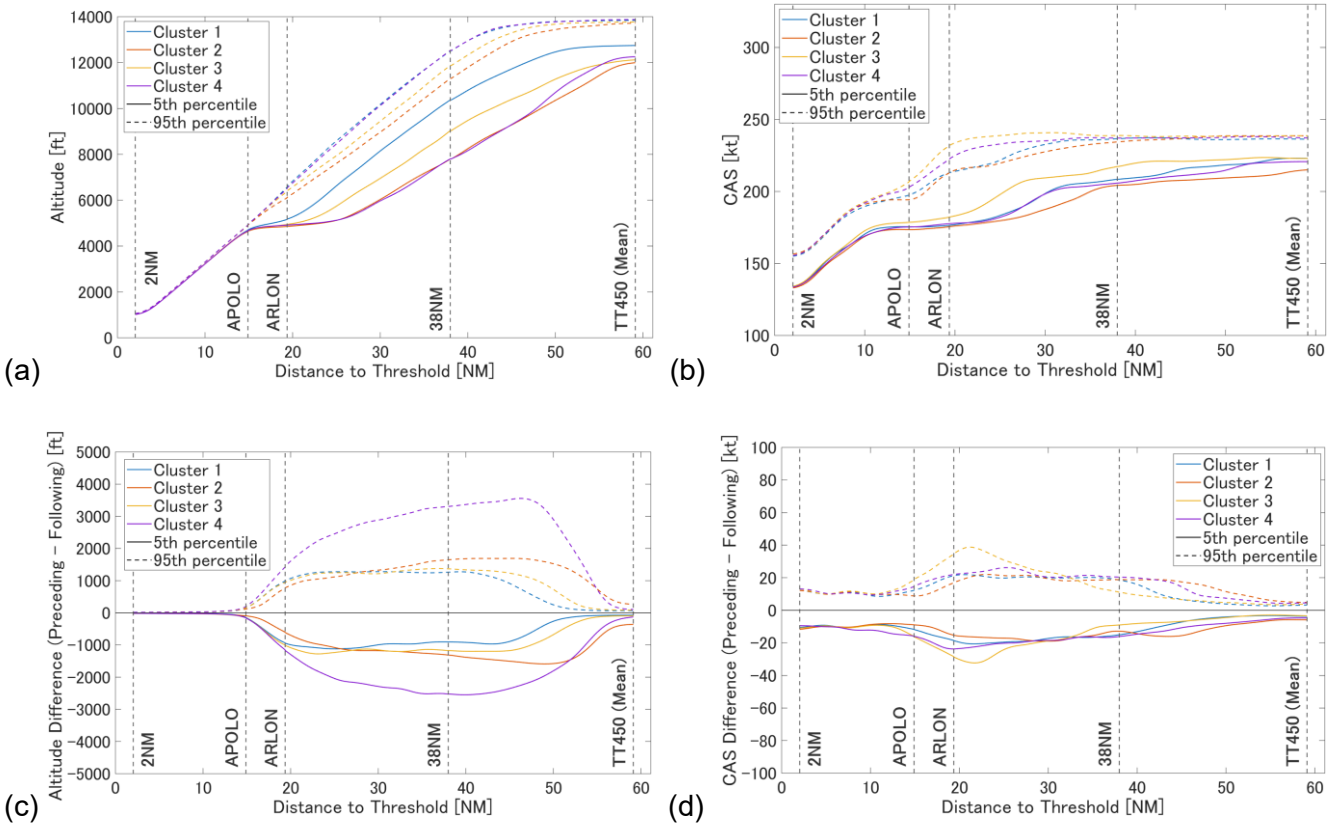


Figure 6 – Cluster-wise trajectory profiles: (a) altitude profiles, (b) CAS profiles, (c) altitude-difference profiles, and (d) CAS-difference profiles.

Figures 6(a) and 6(b) show the distributions of the corresponding altitude profiles and calibrated airspeed (CAS) profiles, respectively. Figures 6(c) and 6(d) show the distributions of the altitude-difference and CAS-difference profiles between preceding and following aircraft, respectively. As in Figure 3, the curves in the figures indicate the 5th and 95th percentiles of the actual trajectories, and approximately 90% of the data lie within this range. As shown in Figures 6(a), the altitude profiles of the preceding and following aircraft in Cluster 1 are relatively similar. This is consistent with Cluster 1 having the smallest values of $S(Alt)$ and ΔAlt, as shown in Table 4. In contrast, in Cluster 4, the altitude difference between the preceding and following aircraft increases markedly from TT450 to around the 38 NM point. Figure 6(c) also shows that the altitude difference reaches approximately 3000 ft or more. Figures 6(b) and 6(d) show that the CAS histories also have different characteristics among the clusters. In Clusters 1 and 2, the CAS differences between preceding and following aircraft are relatively small. In particular, Cluster 2 shows the smallest value of ΔCAS, at 9.41 kt. In contrast, Cluster 3 shows a large CAS difference near ARLON, with the largest ΔCAS value of 13.69 kt. This indicates that Cluster 3 is characterized by relatively small altitude differences but large differences in CAS profiles.

Figures 7(a) and 7(b) show the altitude and calibrated airspeed (CAS) profiles for each cluster, respectively. Figures 7(c) and 7(d) show the altitude-difference and CAS-difference profiles between

preceding and following aircraft, respectively. In addition, Fig. 7(e) shows the distribution of the arrival separation margin for each cluster. As shown in Figures 7(a) and 7(b), the preceding and following aircraft in Cluster 1 have relatively similar altitude and CAS profiles. This tendency is also observed in the difference profiles shown in Figures 7(c) and 7(d), where the variability of the altitude difference is smaller than that in the other clusters. Similarly, the distribution of the arrival separation margin shown in Figures 7(e) indicates that Cluster 1 exhibits limited variability, as reflected by its small standard deviation. In contrast, Cluster 4, which exhibits large variations in altitude and CAS profiles, and Cluster 3, which shows large CAS differences between preceding and following aircraft, exhibit greater variability in the arrival separation margin than the other clusters.

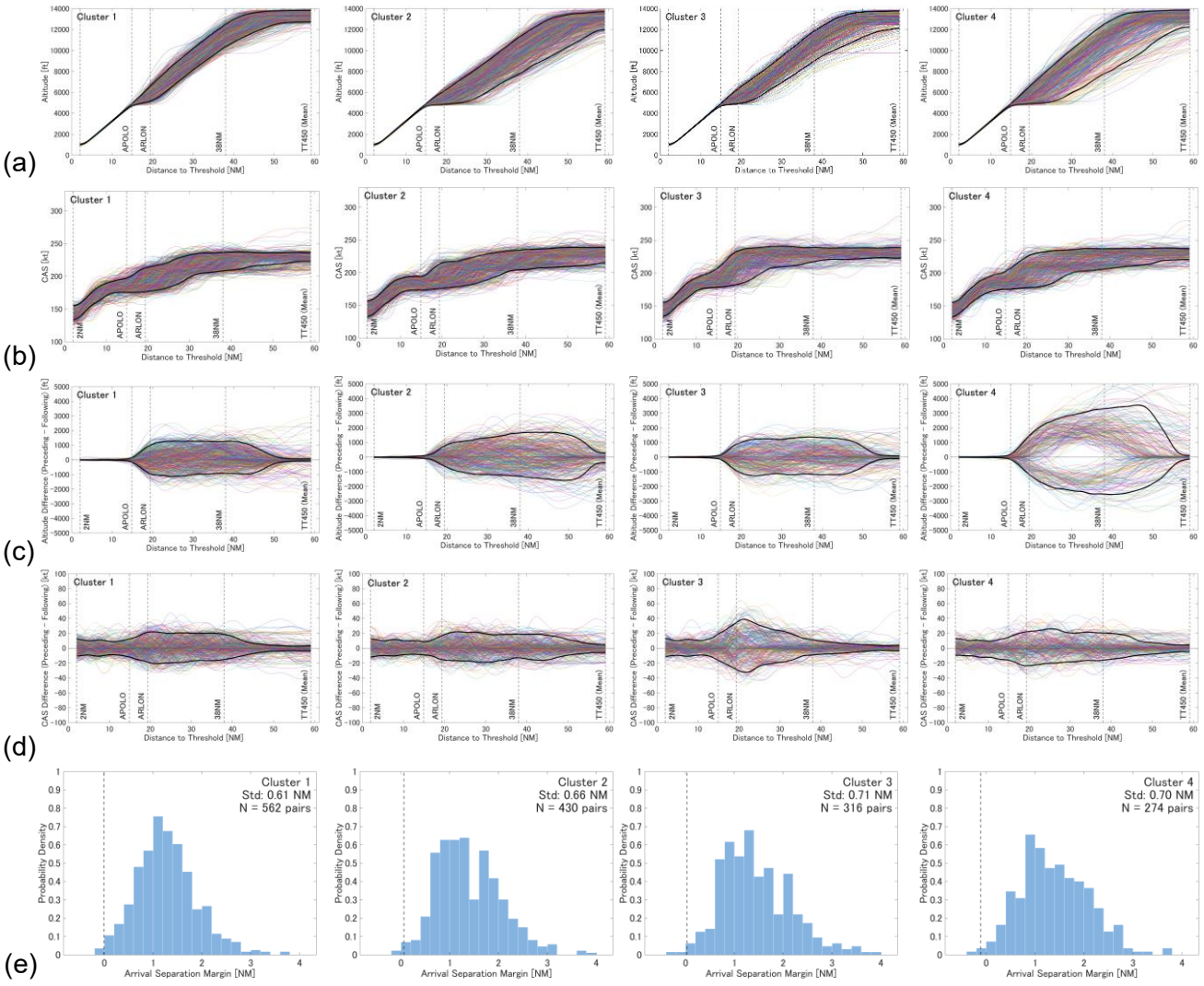


Figure 7 – Cluster-wise trajectory profiles and arrival separation margins:
(a) altitude profiles, (b) CAS profiles, (c) altitude-difference profiles,
(d) CAS-difference profiles, and (e) arrival separation margin distributions.

5.2 Cluster-wise Analysis of Time-Interval Variance Reduction

Figure 8 shows the time-interval distributions between preceding and following aircraft at TT450, 38 NM, APOLO, and 2 NM for each cluster. In the legend, μ and σ^2represent the mean and variance of the time interval at each point, respectively. Figure 9 shows the variation of the time-interval variance between preceding and following aircraft with distance from the runway threshold for each cluster. In addition, Table 5 summarizes the variance at each point and the section-wise changes in variance for each cluster. These results show that the time-interval variance is large near TT450 in all clusters, whereas it decreases markedly from TT450 to 38 NM. These results indicate that the variability in the

time interval between preceding and following aircraft is substantially reduced on the Sequencing Leg. For Clusters 1, 2, and 4, the reductions in time-interval variance from TT450 to 38 NM were $935.5\ s^2$, $967.2\ s^2$, and $1256.9\ s^2$, respectively. These reductions were larger than those observed from 38 NM to APOLO. This indicates that, in these clusters, the variability in the time interval between preceding and following aircraft was mainly reduced by path-length adjustment on the Sequencing Leg. In addition, the time-interval variance at TT450 was largest in Cluster 4, followed by Clusters 2 and 1, and this order remained unchanged until landing. This suggests that the variability in the time interval at the PMS entry point may affect the subsequent variability in arrival separation. In contrast, although Cluster 3 had the smallest variance at TT450, $982.7\ s^2$, its variance at 38 NM remained the largest among all clusters, at $322.0\ s^2$. The reduction in variance from TT450 to 38 NM was$660.7\ s^2$, which was smaller than the reductions observed in the other clusters. In addition, the reduction in variance from 38 NM to APOLO was $125.3\ s^2$, which was the largest among all clusters. This suggests that, in Cluster 3, the effect of path-length adjustment on the Sequencing Leg was relatively small, whereas speed adjustment or other control actions after 38 NM may have contributed to the reduction in time-interval variance. However, the reduction in variance from 38 NM to APOLO was smaller than that from TT450 to 38 NM. Therefore, path-length adjustment on the Sequencing Leg is considered to have made a larger contribution to the reduction in time-interval variance.

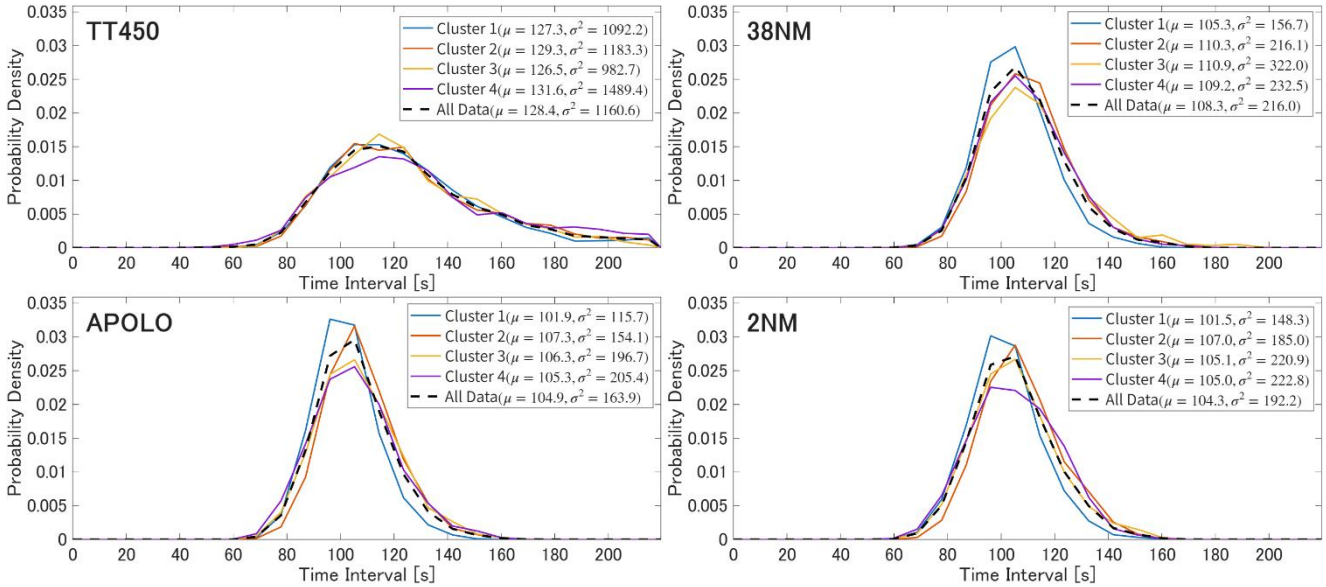


Figure 8 – Cluster-wise time-interval distributions at TT450, 38 NM, APOLO, and 2 NM.

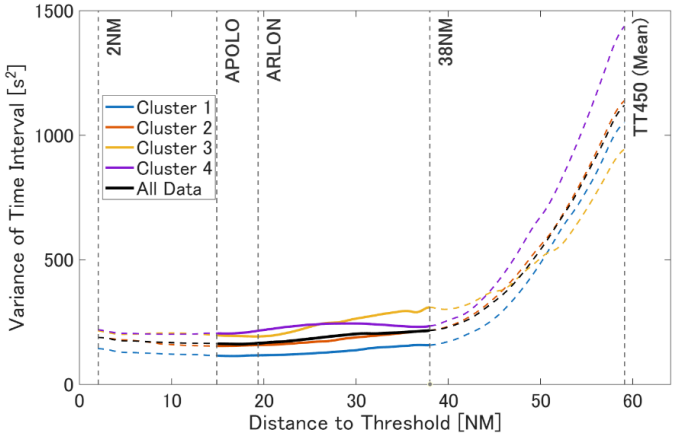


Figure 9 – Cluster-wise time-interval variance as a function of distance to threshold.

Table 5 – Cluster-wise variance reduction rates of time-interval distributions.

j	$\sigma^2_{TT450}\ [s^2]$	$\sigma^2_{38NM}\ [s^2]$	$\sigma^2_{APOLO}\ [s^2]$	$\sigma^2_{2NM}\ [s^2]$	$\sigma^2_{38NM} - \sigma^2_{TT450}[s^2]$	$\sigma^2_{APOLO} - \sigma^2_{38NM}\ [s^2]$	$\sigma^2_{2NM} - \sigma^2_{APOLO}\ [s^2]$
all	1160.6	216.0	163.9	192.2	-944.6	-52.1	+28.3
1	1092.2	156.7	115.7	148.3	-935.5	-41.0	+32.6
2	1183.3	216.1	154.1	185.0	-967.2	-62.0	+30.9
3	982.7	322.0	196.7	220.9	-660.7	-125.3	+24.2
4	1489.4	232.5	205.4	222.8	-1256.9	-27.1	+17.4

6. Conclusion and Future Work

In this study, the feasibility of reducing arrival-separation variability for aircraft arriving at a congested airport via the Point Merge System (PMS) was examined, and the potential to reduce arrival separation while maintaining the current safety level was evaluated. To reduce the influence of differing wind conditions on flight time, clustering based on altitude and CAS profiles was performed for pairs of consecutive arriving aircraft during congested periods. Clusters with low variability in altitude and CAS profiles were identified in the section where no procedural speed or altitude restrictions are specified. The results suggest that lower variations in altitude and CAS profiles are associated with lower arrival-separation variability, indicating the potential for arrival-separation reduction. Under the current traffic condition, the rate of insufficient separation under RECAT may be reduced from approximately 0.54% for the overall dataset to 0.28%. The cluster-wise analysis of time-interval variance also suggested that speed adjustment after leaving the Sequencing Leg may have contributed to reducing time-interval variance in some clusters. However, a quantitative comparison showed that path-length adjustment on the Sequencing Leg contributed more to reducing time-interval variance, and consequently arrival-separation variability, than speed adjustment after leaving the Leg, whose contribution was relatively limited. The differences in time-interval variance at TT450 among clusters further suggest that spacing variability before PMS entry, namely the spacing accuracy established before PMS entry, also influences the stability of final arrival separation.

As future work, it will be necessary to clarify how trajectory variability before PMS entry affects aircraft spacing variability at PMS entry. Another important task is to quantify the variability that would arise when aircraft fly along standardized trajectory profiles under procedural speed and altitude restrictions in PMS operations. This would help further develop the findings of this study toward practical operational implementation.

7. Contact Author Email Address

The contact author Ryo Kajikawa can be reached at the email address shown below:
kajikawa-ryo@ed.tmu.ac.jp

8. Copyright Statement

The authors confirm that they, and/or their company or organization, hold copyright on all of the original material included in this paper. The authors also confirm that they have obtained permission, from the copyright holder of any third party material included in this paper, to publish it as part of their paper. The authors confirm that they give permission, or have obtained permission from the copyright holder of this paper, for the publication and distribution of this paper as part of the ICAS proceedings or as individual off-prints from the proceedings.

References

[1] Civil Aviation Bureau, Ministry of Land, Infrastructure, Transport and Tourism. Current status of domestic aviation (Material 1, 1st Panel of Experts on the Future of Domestic Aviation). https://www.mlit.go.jp/koku/content/001893421.pdf, 2024.

[2] Ministry of Land, Infrastructure, Transport and Tourism. Airport management status: Ranking table by airport for 2024 (calendar year / fiscal year). https://www.mlit.go.jp/koku/15_bf_000185.html, 2025.

[3] Ministry of Land, Infrastructure, Transport and Tourism. Long-term vision for the future air traffic system 2040 (CARATS2040): Challenge to innovative air traffic systems. https://www.mlit.go.jp/koku/carats/rdk40188/wp-content/themes/carats/common/pdf/vision2.pdf, 2025.

[4] EUROCONTROL. Point merge implementation: A quick guide: Simplifying and enhancing arrival operations with closed loop sequencing. 1.51 edition, https://www.eurocontrol.int/publication/point-merge-implementation, 2024.

[5] EUROCONTROL. Tokyo-Haneda, one of the world's busiest airports, set to implement Point Merge, EUROCONTROL's innovative method for sequencing arrival flows. EUROCONTROL, 2019.

[6] Kazama T, Takeichi N and Harada A. An attempt at safety monitoring by analyzing aircraft flight data. Proc 62nd Airplane Symposium, paper number 1D06, 2024.

[7] Kajikawa R and Takeichi N. Feasibility of landing capacity enhancement through arrival trajectory analysis at congested airports. Proc 63rd Airplane Symposium, paper number 1D07, 2025.

[8] Corrado SJ, Puranik TG, Piñon-Fischer OJ and Mavris DN. A clustering-based quantitative analysis of the interdependent relationship between spatial and energy anomalies in ADS-B trajectory data. Transportation Research Part C: Emerging Technologies, Vol. 131, 103331, https://doi.org/10.1016/j.trc.2021.103331, 2021.

[9] Deng C, Choi HC, Park H and Hwang I. Trajectory pattern identification and classification for real-time air traffic applications in Area Navigation terminal airspace. Transportation Research Part C: Emerging Technologies, Vol. 142, 103765, 2022.

[10] Gariel M, Srivastava AN and Feron E. Trajectory clustering and an application to airspace monitoring. IEEE Transactions on Intelligent Transportation Systems, Vol. 12, No. 4, pp 1511-1524, 2011.

[11] OpenSky Network. OpenSky Network website. https://opensky-network.org/.

[12] Research Institute for Sustainable Humano sphere, Kyoto University. Japan Meteorological Agency data. http://database.rish.kyotou.ac.jp/arch/jmadata/data/gpv.

[13] Yoshihara T et al. Wake turbulence control method corresponding to meteorological conditions and its effects. Proc 23rd Electronic Navigation Research Institute Research Conference, 2023.

[14] Japan Aeronautical Information Service Center. AIS JAPAN. Civil Aviation Bureau, Ministry of Land, Infrastructure, Transport and Tourism. Provisions for air navigation services, part 5: Provisions for air traffic control services. 2025.

[15] Aguilera AM and Aguilera-Morillo MC. Penalized PCA approaches for B-spline expansions of smooth functional data. Applied Mathematics and Computation, Vol. 219, No. 14, pp 7805-7819, 2013.

[16] Ward JH Jr. Hierarchical grouping to optimize an objective function. J Am Stat Assoc, vol 58, no 301, pp 236–244, 1963.

[17] Jeddi BG and Shortle JF. Throughput, risk, and economic optimality of runway landing operations. Proc 7th USA/Europe ATM R&D Seminar, Barcelona, Spain, paper number 162, 2007.

[18] Jeddi BG, Shortle JF and Sherry L. Statistical separation standards for the aircraft-approach process. Proc 25th Digital Avionics Systems Conference, pp 2A1-1–2A1-13, 2006.

[19] Sekine K, Kato F, Kageyama K and Itoh E. Data-driven simulation for evaluating the impact of lower arrival aircraft separation on available airspace and runway capacity at Tokyo International Airport. Aerospace, Vol. 8, No. 10, pp 282, 2021.

[20] Jarry G, Delahaye D, Nicol F and Feron E. Aircraft atypical approach detection using functional principal component analysis. Journal of Air Transport Management, Vol. 84, 2020.

[21] Jarry G, Hassoumi A, Delahaye D and Hurter C. Interactive trajectory modification and generation with FPCA. CEAS Aeronautical Journal, 2022.

[22] Chen J, Wang J, Li F and Zou L. Impact of rainy season on approach trajectories in high-altitude airport terminal maneuvering area: a clustering analysis. Scientific Reports, Vol. 15, Article no. 30455, 2025.

[23] Hirabayashi H, Brown M and Takeichi N. Study of a representative wind selection method using track data to evaluate Pacific flight operations. Journal of Air Transport Management, Vol. 119, Article no. 102639, 2024.

[24] Calinski T and Harabasz J. A dendrite method for cluster analysis. Communications in Statistics, Vol. 3, No. 1, pp 1–27, 1974.